



# CHORUS

This is the accepted manuscript made available via CHORUS. The article has been published as:

## Observation of $Z_{\{b\}}(10610)$ and $Z_{\{b\}}(10650)$ Decaying to B Mesons

A. Garmash *et al.* (Belle Collaboration)

Phys. Rev. Lett. **116**, 212001 — Published 24 May 2016

DOI: [10.1103/PhysRevLett.116.212001](https://doi.org/10.1103/PhysRevLett.116.212001)

## Study of $e^+e^- \rightarrow B^{(*)}\bar{B}^{(*)}\pi^\pm$ at $\sqrt{s} = 10.866$ GeV

A. Garmash,<sup>3,47</sup> A. Abdesselam,<sup>57</sup> I. Adachi,<sup>13,10</sup> H. Aihara,<sup>62</sup> D. M. Asner,<sup>49</sup> T. Aushev,<sup>38</sup> R. Ayad,<sup>57</sup> T. Aziz,<sup>58</sup>  
V. Babu,<sup>58</sup> I. Badhrees,<sup>57,26</sup> A. M. Bakich,<sup>56</sup> P. Behera,<sup>17</sup> V. Bhardwaj,<sup>54</sup> B. Bhuyan,<sup>16</sup> A. Bobrov,<sup>3,47</sup>  
A. Bondar,<sup>3,47</sup> G. Bonvicini,<sup>67</sup> A. Bozek,<sup>45</sup> M. Bračko,<sup>34,22</sup> T. E. Browder,<sup>12</sup> D. Červenkov,<sup>4</sup> V. Chekelian,<sup>35</sup>  
A. Chen,<sup>42</sup> B. G. Cheon,<sup>11</sup> K. Chilikin,<sup>37</sup> K. Cho,<sup>27</sup> V. Chobanova,<sup>35</sup> Y. Choi,<sup>55</sup> D. Cinabro,<sup>67</sup> J. Dalseno,<sup>35,59</sup>  
M. Danilov,<sup>37</sup> N. Dash,<sup>15</sup> Z. Doležal,<sup>4</sup> A. Drutskoy,<sup>37</sup> D. Dutta,<sup>58</sup> S. Eidelman,<sup>3,47</sup> D. Epifanov,<sup>62</sup> H. Farhat,<sup>67</sup>  
J. E. Fast,<sup>49</sup> T. Ferber,<sup>7</sup> B. G. Fulsom,<sup>49</sup> V. Gaur,<sup>58</sup> N. Gabyshev,<sup>3,47</sup> R. Gillard,<sup>67</sup> Y. M. Goh,<sup>11</sup> P. Goldenzweig,<sup>24</sup>  
B. Golob,<sup>31,22</sup> T. Hara,<sup>13,10</sup> K. Hayasaka,<sup>40</sup> H. Hayashii,<sup>41</sup> T. Iijima,<sup>40,39</sup> A. Ishikawa,<sup>60</sup> R. Itoh,<sup>13,10</sup> Y. Iwasaki,<sup>13</sup>  
I. Jaegle,<sup>12</sup> D. Joffe,<sup>25</sup> K. K. Joo,<sup>5</sup> T. Julius,<sup>36</sup> K. H. Kang,<sup>29</sup> E. Kato,<sup>60</sup> T. Kawasaki,<sup>46</sup> D. Y. Kim,<sup>53</sup> J. B. Kim,<sup>28</sup>  
K. T. Kim,<sup>28</sup> M. J. Kim,<sup>29</sup> S. H. Kim,<sup>11</sup> Y. J. Kim,<sup>27</sup> K. Kinoshita,<sup>6</sup> S. Korpar,<sup>34,22</sup> P. Križan,<sup>31,22</sup> P. Krokovny,<sup>3,47</sup>  
T. Kuhr,<sup>32</sup> A. Kuzmin,<sup>3,47</sup> Y.-J. Kwon,<sup>69</sup> J. S. Lange,<sup>9</sup> I. S. Lee,<sup>11</sup> C. Li,<sup>36</sup> H. Li,<sup>18</sup> L. Li,<sup>51</sup> L. Li Gioi,<sup>35</sup> J. Libby,<sup>17</sup>  
D. Liventsev,<sup>66,13</sup> P. Lukin,<sup>3,47</sup> M. Masuda,<sup>61</sup> D. Matvienko,<sup>3,47</sup> K. Miyabayashi,<sup>41</sup> H. Miyata,<sup>46</sup> R. Mizuk,<sup>37,38</sup>  
G. B. Mohanty,<sup>58</sup> A. Moll,<sup>35,59</sup> T. Mori,<sup>39</sup> R. Mussa,<sup>21</sup> E. Nakano,<sup>48</sup> M. Nakao,<sup>13,10</sup> T. Nanut,<sup>22</sup> Z. Natkaniec,<sup>45</sup>  
S. Nishida,<sup>13,10</sup> S. L. Olsen,<sup>52</sup> P. Pakhlov,<sup>37</sup> G. Pakhlova,<sup>38</sup> B. Pal,<sup>6</sup> H. Park,<sup>29</sup> T. K. Pedlar,<sup>33</sup> R. Pestotnik,<sup>22</sup>  
M. Petrič,<sup>22</sup> L. E. Pilonen,<sup>66</sup> C. Pulvermacher,<sup>24</sup> E. RIBEŽL,<sup>22</sup> M. Ritter,<sup>35</sup> A. Rostomyan,<sup>7</sup> H. Sahoo,<sup>12</sup>  
Y. Sakai,<sup>13,10</sup> S. Sandilya,<sup>58</sup> T. Sanuki,<sup>60</sup> V. Savinov,<sup>50</sup> O. Schneider,<sup>30</sup> G. Schnell,<sup>1,14</sup> C. Schwanda,<sup>20</sup> Y. Seino,<sup>46</sup>  
D. Semmler,<sup>9</sup> K. Senyo,<sup>68</sup> I. S. Seong,<sup>12</sup> M. E. Seviar,<sup>36</sup> V. Shebalin,<sup>3,47</sup> C. P. Shen,<sup>2</sup> T.-A. Shibata,<sup>63</sup> J.-G. Shiu,<sup>44</sup>  
B. Shwartz,<sup>3,47</sup> F. Simon,<sup>35,59</sup> Y.-S. Sohn,<sup>69</sup> E. Solovieva,<sup>38</sup> M. Starič,<sup>22</sup> T. Sumiyoshi,<sup>64</sup> U. Tamponi,<sup>21,65</sup>  
K. Tanida,<sup>52</sup> Y. Teramoto,<sup>48</sup> K. Trabelsi,<sup>13,10</sup> M. Uchida,<sup>63</sup> S. Uehara,<sup>13,10</sup> T. Uglov,<sup>38</sup> S. Uno,<sup>13,10</sup>  
C. Van Hulse,<sup>1</sup> P. Vanhoefer,<sup>35</sup> G. Varner,<sup>12</sup> V. Vorobyev,<sup>3,47</sup> M. N. Wagner,<sup>9</sup> C. H. Wang,<sup>43</sup> M.-Z. Wang,<sup>44</sup>  
P. Wang,<sup>19</sup> Y. Watanabe,<sup>23</sup> K. M. Williams,<sup>66</sup> E. Won,<sup>28</sup> H. Yamamoto,<sup>60</sup> J. Yamaoka,<sup>49</sup> S. Yashchenko,<sup>7</sup>  
J. Yelton,<sup>8</sup> Y. Yook,<sup>69</sup> C. Z. Yuan,<sup>19</sup> Z. P. Zhang,<sup>51</sup> V. Zhilich,<sup>3,47</sup> V. Zhulanov,<sup>3,47</sup> and A. Zupanc<sup>22</sup>

(The Belle Collaboration)

<sup>1</sup>University of the Basque Country UPV/EHU, 48080 Bilbao

<sup>2</sup>Beihang University, Beijing 100191

<sup>3</sup>Budker Institute of Nuclear Physics SB RAS, Novosibirsk 630090

<sup>4</sup>Faculty of Mathematics and Physics, Charles University, 121 16 Prague

<sup>5</sup>Chonnam National University, Kwangju 660-701

<sup>6</sup>University of Cincinnati, Cincinnati, Ohio 45221

<sup>7</sup>Deutsches Elektronen-Synchrotron, 22607 Hamburg

<sup>8</sup>University of Florida, Gainesville, Florida 32611

<sup>9</sup>Justus-Liebig-Universität Gießen, 35392 Gießen

<sup>10</sup>SOKENDAI (The Graduate University for Advanced Studies), Hayama 240-0193

<sup>11</sup>Hanyang University, Seoul 133-791

<sup>12</sup>University of Hawaii, Honolulu, Hawaii 96822

<sup>13</sup>High Energy Accelerator Research Organization (KEK), Tsukuba 305-0801

<sup>14</sup>IKERBASQUE, Basque Foundation for Science, 48013 Bilbao

<sup>15</sup>Indian Institute of Technology Bhubaneswar, Satya Nagar 751007

<sup>16</sup>Indian Institute of Technology Guwahati, Assam 781039

<sup>17</sup>Indian Institute of Technology Madras, Chennai 600036

<sup>18</sup>Indiana University, Bloomington, Indiana 47408

<sup>19</sup>Institute of High Energy Physics, Chinese Academy of Sciences, Beijing 100049

<sup>20</sup>Institute of High Energy Physics, Vienna 1050

<sup>21</sup>INFN - Sezione di Torino, 10125 Torino

<sup>22</sup>J. Stefan Institute, 1000 Ljubljana

<sup>23</sup>Kanagawa University, Yokohama 221-8686

<sup>24</sup>Institut für Experimentelle Kernphysik, Karlsruher Institut für Technologie, 76131 Karlsruhe

<sup>25</sup>Kennesaw State University, Kennesaw GA 30144

<sup>26</sup>King Abdulaziz City for Science and Technology, Riyadh 11442

<sup>27</sup>Korea Institute of Science and Technology Information, Daejeon 305-806

<sup>28</sup>Korea University, Seoul 136-713

<sup>29</sup>Kyungpook National University, Daegu 702-701

<sup>30</sup>École Polytechnique Fédérale de Lausanne (EPFL), Lausanne 1015

<sup>31</sup>Faculty of Mathematics and Physics, University of Ljubljana, 1000 Ljubljana

- 56 <sup>32</sup>Ludwig Maximilians University, 80539 Munich  
57 <sup>33</sup>Luther College, Decorah, Iowa 52101  
58 <sup>34</sup>University of Maribor, 2000 Maribor  
59 <sup>35</sup>Max-Planck-Institut für Physik, 80805 München  
60 <sup>36</sup>School of Physics, University of Melbourne, Victoria 3010  
61 <sup>37</sup>Moscow Physical Engineering Institute, Moscow 115409  
62 <sup>38</sup>Moscow Institute of Physics and Technology, Moscow Region 141700  
63 <sup>39</sup>Graduate School of Science, Nagoya University, Nagoya 464-8602  
64 <sup>40</sup>Kobayashi-Maskawa Institute, Nagoya University, Nagoya 464-8602  
65 <sup>41</sup>Nara Women's University, Nara 630-8506  
66 <sup>42</sup>National Central University, Chung-li 32054  
67 <sup>43</sup>National United University, Miao Li 36003  
68 <sup>44</sup>Department of Physics, National Taiwan University, Taipei 10617  
69 <sup>45</sup>H. Niewodniczanski Institute of Nuclear Physics, Krakow 31-342  
70 <sup>46</sup>Niigata University, Niigata 950-2181  
71 <sup>47</sup>Novosibirsk State University, Novosibirsk 630090  
72 <sup>48</sup>Osaka City University, Osaka 558-8585  
73 <sup>49</sup>Pacific Northwest National Laboratory, Richland, Washington 99352  
74 <sup>50</sup>University of Pittsburgh, Pittsburgh, Pennsylvania 15260  
75 <sup>51</sup>University of Science and Technology of China, Hefei 230026  
76 <sup>52</sup>Seoul National University, Seoul 151-742  
77 <sup>53</sup>Soongsil University, Seoul 156-743  
78 <sup>54</sup>University of South Carolina, Columbia, South Carolina 29208  
79 <sup>55</sup>Sungkyunkwan University, Suwon 440-746  
80 <sup>56</sup>School of Physics, University of Sydney, NSW 2006  
81 <sup>57</sup>Department of Physics, Faculty of Science, University of Tabuk, Tabuk 71451  
82 <sup>58</sup>Tata Institute of Fundamental Research, Mumbai 400005  
83 <sup>59</sup>Excellence Cluster Universe, Technische Universität München, 85748 Garching  
84 <sup>60</sup>Tohoku University, Sendai 980-8578  
85 <sup>61</sup>Earthquake Research Institute, University of Tokyo, Tokyo 113-0032  
86 <sup>62</sup>Department of Physics, University of Tokyo, Tokyo 113-0033  
87 <sup>63</sup>Tokyo Institute of Technology, Tokyo 152-8550  
88 <sup>64</sup>Tokyo Metropolitan University, Tokyo 192-0397  
89 <sup>65</sup>University of Torino, 10124 Torino  
90 <sup>66</sup>CNP, Virginia Polytechnic Institute and State University, Blacksburg, Virginia 24061  
91 <sup>67</sup>Wayne State University, Detroit, Michigan 48202  
92 <sup>68</sup>Yamagata University, Yamagata 990-8560  
93 <sup>69</sup>Yonsei University, Seoul 120-749

We report the analysis of the three-body  $e^+e^- \rightarrow B\bar{B}\pi^\pm$ ,  $B\bar{B}^*\pi^\pm$ , and  $B^*\bar{B}^*\pi^\pm$  processes, including the first observations of the  $Z_b^\pm(10610) \rightarrow [B\bar{B}^* + \text{c.c.}]^\pm$  and  $Z_b^\pm(10650) \rightarrow [B^*\bar{B}^*]^\pm$  transitions that are found to dominate the corresponding final states. We measure Born cross sections for the three-body production of  $\sigma(e^+e^- \rightarrow [B\bar{B}^* + \text{c.c.}]^\pm\pi^\mp) = (17.4 \pm 1.6(\text{stat.}) \pm 1.9(\text{syst.}))$  pb and  $\sigma(e^+e^- \rightarrow [B^*\bar{B}^*]^\pm\pi^\mp) = (8.75 \pm 1.15(\text{stat.}) \pm 1.04(\text{syst.}))$  pb and set a 90% C.L. upper limit of  $\sigma(e^+e^- \rightarrow [B\bar{B}]^\pm\pi^\mp) < 2.9$  pb. The results are based on a 121.4 fb<sup>-1</sup> data sample collected with the Belle detector at a center-of-mass energy near the  $\Upsilon(10860)$  peak.

94 PACS numbers: 14.40.Rt, 14.40.Pq, 13.66.Bc

95 Two new charged bottomonium-like resonances,<sup>107</sup>  
96  $Z_b(10610)$  and  $Z_b(10650)$ , have been observed recently<sup>108</sup>  
97 by the Belle Collaboration in  $e^+e^- \rightarrow \Upsilon(nS)\pi^+\pi^-$ ,  
98  $n = 1, 2, 3$  and  $e^+e^- \rightarrow h_b(mP)\pi^+\pi^-$ ,  $m = 1, 2$  [1, 2].<sup>109</sup>  
99 Analysis of the quark composition of the initial and final<sup>110</sup>  
100 states reveals that these hadronic objects have an exotic<sup>111</sup>  
101 nature:  $Z_b$  should be comprised of (at least) four quarks<sup>112</sup>  
102 including a  $b\bar{b}$  pair. Several models [3] have been pro-<sup>113</sup>  
103 posed to describe the internal structure of these states. In<sup>114</sup>  
104 Ref. [4], it was suggested that  $Z_b(10610)$  and  $Z_b(10650)$ <sup>115</sup>  
105 states might be loosely bound  $B\bar{B}^*$  and  $B^*\bar{B}^*$  systems,<sup>116</sup>  
106 respectively. If so, it is natural to expect the  $Z_b$  states<sup>117</sup>

to decay to final states with  $B^{(*)}$  mesons at substantial rates.

Evidence for the three-body  $\Upsilon(10860) \rightarrow B\bar{B}^*\pi$  decay has been reported previously by Belle, based on a data sample of 23.6 fb<sup>-1</sup> [5]. In this analysis, we use a data sample with an integrated luminosity of 121.4 fb<sup>-1</sup> collected near the peak of the  $\Upsilon(10860)$  resonance ( $\sqrt{s} = 10.866$  GeV) with the Belle detector [6] at the KEKB asymmetric-energy  $e^+e^-$  collider [7]. Note that we reconstruct only three-body  $B^{(*)}\bar{B}^{(*)}\pi$  combinations with a charged primary pion. For brevity, we adopt the following notations: the set of  $B^+\bar{B}^0\pi^-$  and

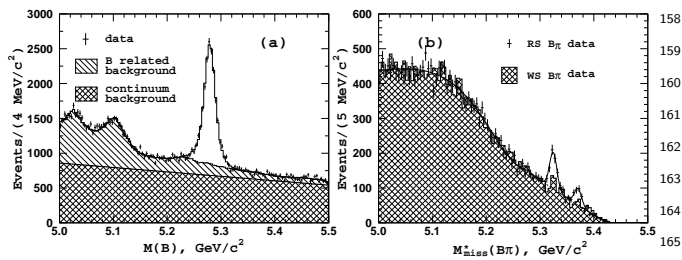


FIG. 1: The (a) invariant mass and (b)  $M_{\text{miss}}^*(B\pi)$  distribu-  
tion for  $B$  candidates in the  $B$  signal region. Points with error  
bars represent the data. The open histogram in (a) shows the  
result of the fit to data. The solid line in (b) shows the result  
of the fit to the RS  $B\pi$  data; the dashed line represents the  
background level.

ing variables that characterize the event topology. Since  
the momenta of the two  $B$  mesons produced from a three-  
body  $e^+e^- \rightarrow B^{(*)}B^{(*)}\pi$  decay are low in the center-of-  
mass (c.m.) frame (below  $0.9 \text{ GeV}/c$ ), the decay prod-  
ucts of different  $B$  mesons are essentially uncorrelated so  
that the event tends to be spherical. In contrast, hadrons  
from continuum events tend to exhibit a back-to-back jet  
structure. We use  $\theta_{\text{thr}}$ , the angle between the thrust axis  
of the  $B$  candidate and that of the rest of the event, to  
discriminate between the two cases. The distribution of  
 $|\cos\theta_{\text{thr}}|$  is strongly peaked near  $|\cos\theta_{\text{thr}}| = 1.0$  for  $c\bar{c}$   
events and is nearly flat for  $B^{(*)}B^{(*)}\pi$  events. We re-  
quire  $|\cos\theta_{\text{thr}}| < 0.80$  for the  $B \rightarrow D^{(*)}\pi$  final states;  
this eliminates about 81% of the continuum background  
and retains 73% of the signal events.

We identify  $B$  candidates by their reconstructed in-  
variant mass  $M(B)$  and momentum  $P(B)$  in the c.m.  
frame. We require  $P(B) < 1.35 \text{ GeV}/c$  to retain  $B$   
mesons produced in both two-body and multibody pro-  
cesses. The  $M(B)$  distribution for  $B$  candidates is shown  
in Fig. 1(a). We perform a binned maximum likelihood  
fit of the  $M(B)$  distribution to the sum of a signal compo-  
nent parameterized by a Gaussian function and two back-  
ground components: one related to other decay modes of  
 $B$  mesons and one due to continuum  $e^+e^- \rightarrow q\bar{q}$  pro-  
cesses, where  $q = u, d, s, c$ . The shape of the  $B$ -related  
background is determined from a large sample of generic  
MC; the shape of the  $q\bar{q}$  background is parameterized  
with a linear function. The parameters of the signal  
Gaussian, the normalization of the  $B$ -related background  
and the parameters of the  $q\bar{q}$  background float in the fit.  
We find  $12263 \pm 168$  fully reconstructed  $B$  mesons. The  
 $B$  signal region is defined by requiring  $M(B)$  to be within  
30 to 40  $\text{MeV}/c^2$  (depending on the  $B$  decay mode) of  
the nominal  $B$  mass.

Reconstructed  $B^+$  or  $\bar{B}^0$  candidates are combined with  
 $\pi^-$ 's — the right-sign (RS) combination — and the  
missing mass,  $M_{\text{miss}}(B\pi)$ , is calculated as  $M_{\text{miss}}(B\pi) =$   
 $\sqrt{(\sqrt{s} - E_{B\pi})^2/c^4 - P_{B\pi}^2/c^2}$ , where  $E_{B\pi}$  and  $P_{B\pi}$  are  
the measured energy and momentum of the reconstructed  
 $B\pi$  combination. Signal  $e^+e^- \rightarrow BB^*\pi$  events produce  
a narrow peak in the  $M_{\text{miss}}(B\pi)$  spectrum around the  
nominal  $B^*$  mass while  $e^+e^- \rightarrow B^*B^*\pi$  events produce  
a peak at  $m_{B^*} + \Delta m_{B^*}$ , where  $\Delta m_{B^*} = m_{B^*} - m_B$ ,  
due to the missed photon from the  $B^* \rightarrow B\gamma$  decay. It  
is important to note here that, according to signal MC,  
 $BB^*\pi$  events, where the reconstructed  $B$  is the one from  
the  $B^*$ , produce a peak in the  $M_{\text{miss}}(B\pi)$  distribution at  
virtually the same position as  $BB^*\pi$  events, where the  
reconstructed  $B$  is the primary one. To remove the cor-  
relation between  $M_{\text{miss}}(B\pi)$  and  $M(B)$  and to improve  
the resolution, we use  $M_{\text{miss}}^* = M_{\text{miss}}(B\pi) + M(B) - m_B$   
instead of  $M_{\text{miss}}(B\pi)$ . The  $M_{\text{miss}}^*$  distribution for the RS  
combinations is shown in Fig. 1(b), where peaks corre-  
sponding to the  $BB^*\pi$  and  $B^*B^*\pi$  signals are evident.  
Combinations with  $\pi^+$  — the wrong sign (WS) combi-

$B^-B^0\pi^+$  final states is referred to as  $BB\pi$ ; the set of  
 $B^+B^*0\pi^-$ ,  $B^-B^*0\pi^+$ ,  $B^0B^*\pi^-$  and  $\bar{B}^0B^*\pi^-$  final  
states is referred to as  $BB^*\pi$ ; and the set of  $B^{*+}\bar{B}^*0\pi^-$   
and  $B^{*-}B^*0\pi^+$  final states is denoted as  $B^*B^*\pi$ . The in-  
clusion of the charge conjugate mode is implied through-  
out this report.

We use Monte Carlo (MC) events generated with Evt-  
Gen [8] and then processed through a detailed detector  
simulation implemented in GEANT3 [9]. The simulated  
samples for  $e^+e^- \rightarrow q\bar{q}$  ( $q = u, d, s, c$ , or  $b$ ) are equiv-  
alent to six times the integrated luminosity of the data  
and are used to develop criteria to separate signal events  
from backgrounds, identify types of background events,  
determine the reconstruction efficiency and parameterize  
the distributions needed for the extraction of the signal  
decays.

$B$  mesons are reconstructed in the following decay  
channels:  $B^+ \rightarrow J/\psi K^{(*)+}$ ,  $B^+ \rightarrow \bar{D}^{(*)0}\pi^+$ ,  $B^0 \rightarrow$   
 $J/\psi K^{(*)0}$ ,  $B^0 \rightarrow D^{(*)-}\pi^+$ . We use Belle standard tech-  
niques [10] to reconstruct primary particles such as pho-  
tons, pions, kaons, and leptons. The  $K^{*0}$  ( $K^{*+}$ ) is re-  
constructed in the  $K^+\pi^-$  ( $K^0\pi^+$ ) final state; the invari-  
ant mass of the  $K^*$  candidate is required to be within  
150  $\text{MeV}/c^2$  of the nominal  $K^*$  mass [11]. The invari-  
ant mass of a  $J/\psi \rightarrow \ell^+\ell^-$  candidate is required to  
be within 30 (50)  $\text{MeV}/c^2$  for  $\ell = e$  ( $\mu$ ), of the nom-  
inal  $J/\psi$  mass. Neutral (charged)  $D$  mesons are re-  
constructed in the  $K^-\pi^+$ ,  $K^-\pi^+\pi^0$ , and  $K^-\pi^-\pi^+\pi^+$   
( $K^-\pi^+\pi^+$ ) modes. To identify  $D^*$  candidates, we require  
 $|M(D\pi) - M(D) - \Delta m_{D^*}| < 3 \text{ MeV}/c^2$ , where  $M(D\pi)$   
and  $M(D)$  are the reconstructed masses of the  $D^*$  and  
 $D$  candidates, respectively, and  $\Delta m_{D^*} = m_{D^*} - m_D$  is the  
difference between the nominal  $D^*$  and  $D$  masses. The  
mass windows for narrow states quoted above correspond  
to a  $\pm 2.5\sigma$  requirement.

The dominant background comes from  $e^+e^- \rightarrow c\bar{c}$  con-  
tinuum events, where true  $D$  mesons produced in  $e^+e^-$   
annihilation are combined with random particles to form  
a  $B$  candidate. This type of background is suppressed us-

nations — are used to evaluate the shape of the combinatorial background. (The  $B \rightarrow J/\psi K^0$  mode is not included in the WS sample but both combinations with  $\pi^+$  and  $\pi^-$  are added to the RS sample.) We apply factor of  $1.19 \pm 0.01$  [12] to the WS distribution to normalize it to the expected number of the background events in the RS sample. There is also a hint for a peaking structure in the WS  $M_{\text{miss}}^*$  distribution, shown as a hatched histogram in Fig. 1(b). Due to  $B^0 - \bar{B}^0$  oscillations, we expect a fraction of the produced  $B^0$  mesons to decay as  $\bar{B}^0$  given by  $0.5x_d^2/(1+x_d^2) = 0.1861 \pm 0.0024$ , where  $x_d$  is the  $B^0$  mixing parameter [11].

Note that the momentum spectrum of  $B$  mesons produced in events with initial-state radiation (ISR),  $e^+e^- \rightarrow \gamma B\bar{B}$ , overlaps significantly with that for  $B$  mesons from the three-body  $e^+e^- \rightarrow B^{(*)}B^{(*)}\pi$  processes. However, ISR events do not produce peaking structures in the  $M_{\text{miss}}^*$  distribution.

A binned maximum likelihood fit is performed to fit the  $M_{\text{miss}}^*$  distribution to the sum of three Gaussian functions to represent three possible signals and two threshold components  $A_k(x_k - M_{\text{miss}}^*)^{\alpha_k} \exp\{(M_{\text{miss}}^* - x_k)/\delta_k\}$  ( $k = 1, 2$ ) to parameterize the  $q\bar{q}$  and two-body  $B^{(*)}B^{(*)}$  backgrounds. The means and widths of the signal Gaussian functions are fixed from the signal MC simulation. The parameters  $A_k$ ,  $\alpha_k$ ,  $\delta_k$  of the background functions are free parameters of the fit; the threshold parameters  $x_k$  are fixed from the generic MC. ISR events produce an  $M_{\text{miss}}^*$  distribution similar to that for  $q\bar{q}$  events; these two components are modeled by a single threshold function. The resolution of the signal peaks in Fig. 1(b) is dominated by the c.m. energy spread and is fixed at  $6.5 \text{ MeV}/c^2$  and  $6.2 \text{ MeV}/c^2$  for the  $BB^*\pi$  and  $B^*B^*\pi$ , respectively as determined from the signal MC. The fit to the RS spectrum yields  $N_{BB^*\pi} = 13 \pm 25$ ,  $N_{BB^*\pi} = 357 \pm 30$  and  $N_{B^*B^*\pi} = 161 \pm 21$  signal events. The statistical significance of the observed  $BB^*\pi$  and  $B^*B^*\pi$  signal is  $9.3\sigma$  and  $8.1\sigma$ , respectively. The statistical significance is calculated as  $\sqrt{-2\ln(\mathcal{L}_0/\mathcal{L}_{\text{sig}})}$ , where  $\mathcal{L}_{\text{sig}}$  and  $\mathcal{L}_0$  denote the likelihood values obtained with the nominal fit and with the signal yield fixed at zero, respectively.

For the subsequent analysis, we require  $|M_{\text{miss}}^* - m_{B^*}| < 15 \text{ MeV}/c^2$  to select  $BB^*\pi$  signal events and  $|M_{\text{miss}}^* - (m_{B^*} + \Delta m_B)| < 12 \text{ MeV}/c^2$ , where  $\Delta m_B = m_{B^*} - m_B$ , to select  $B^*B^*\pi$  events. For the selected  $B^{(*)}B^*\pi$  candidates, we calculate  $M_{\text{miss}}(\pi) = \sqrt{(\sqrt{s} - E_\pi)^2/c^4 - P_\pi^2/c^2}$ , where  $E_\pi$  and  $P_\pi$  are the reconstructed energy and momentum, respectively, of the charged pion in the c.m. frame. The  $M_{\text{miss}}(\pi)$  distributions are shown in Fig. 2 [13]. We perform a simultaneous binned maximum likelihood fit to the RS and WS samples, assuming the same number (after normalization) and distribution of background events in both samples and known fraction of signal events in the RS sample that leaks to the WS sample due to mixing. To fit the

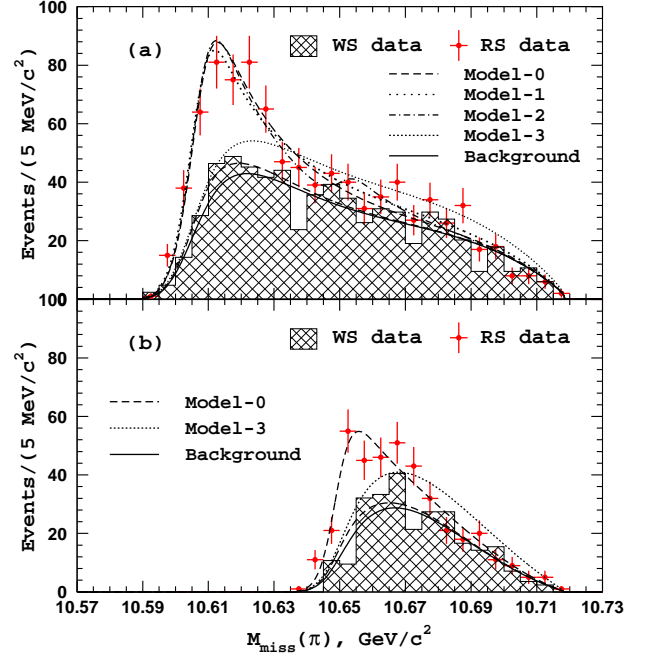


FIG. 2: The  $M_{\text{miss}}(\pi)$  distribution for the (a)  $BB^*\pi$  and (b)  $B^*B^*\pi$  candidate events. Normalization factor is applied for the WS distributions.

$M_{\text{miss}}(\pi)$  spectrum, we use the function

$$F(m) = [f_{\text{sig}}S(m) + B(m)]\epsilon(m)F_{\text{PHSP}}(m), \quad (1)$$

where  $m \equiv M_{\text{miss}}(\pi)$ ;  $f_{\text{sig}} = 1.0$  ( $0.1366 \pm 0.0032$ , [14]) for the RS (WS) sample;  $S(m)$  and  $B(m)$  are the signal and background PDFs, respectively; and  $F_{\text{PHSP}}(m)$  is the phase space function. To account for the instrumental resolution, we smear the function  $F(m)$  with a Gaussian function with  $\sigma = 6.0 \text{ MeV}/c^2$  that is dominated by the c.m. energy spread. The reconstruction efficiency is parametrized as  $\epsilon(m) \sim \exp((m - m_0)/\Delta)(1 - m/m_0)^{3/4}$ , where  $m_0 = 10.718 \pm 0.001 \text{ GeV}/c^2$  is an efficiency threshold and  $\Delta = 0.094 \pm 0.002 \text{ GeV}/c^2$ .

The distribution of background events is parameterized as  $B_{B^{(*)}B^*\pi}(m) = b_0 e^{-\beta\delta_m}$ , where  $b_0$  and  $\beta$  are fit parameters and  $\delta_m = m - (m_{B^{(*)}} + m_{B^*})$ . A general form of the signal PDF is written as

$$S(m) = |\mathcal{A}_{Z_b(10610)} + \mathcal{A}_{Z_b(10650)} + \mathcal{A}_{\text{nr}}|^2, \quad (2)$$

where  $\mathcal{A}_{\text{nr}} = a_{\text{nr}} e^{i\phi_{\text{nr}}}$  is the non-resonant amplitude parameterized as a complex constant and the two  $Z_b$  amplitudes,  $\mathcal{A}_{Z_b}$ , are parameterized with Breit-Wigner functions  $\mathcal{A}_{Z_b} = a_Z e^{i\phi_Z} / (m^2 - m_Z^2 - i\Gamma_Z m_Z)$ . The masses and widths of the  $Z_b$  states are fixed at the values obtained from the analyses of  $e^+e^- \rightarrow \Upsilon(nS)\pi^+\pi^-$  and  $e^+e^- \rightarrow h_b(m_P)\pi^+\pi^-$ :  $M_{Z_b(10610)} = 10607.2 \pm 2.0 \text{ MeV}/c^2$ ,  $\Gamma_{Z_b(10610)} = 18.4 \pm 2.4 \text{ MeV}$  and  $M_{Z_b(10650)} = 10652.2 \pm 1.5 \text{ MeV}/c^2$ ,  $\Gamma_{Z_b(10650)} = 11.5 \pm 2.2 \text{ MeV}$  [1].

TABLE I: Summary of fit results to the  $M_{\text{miss}}(\pi)$  distributions for the three-body  $BB^*\pi$  and  $B^*B^*\pi$  final states.

Mode	Parameter	Model-0	Model-1		Model-2		Model-3
			Solution 1	Solution 2	Solution 1	Solution 2	
$BB^*\pi$	$f_{Z_b(10610)}$	1.0	$1.45 \pm 0.24$	$0.64 \pm 0.15$	$1.01 \pm 0.13$	$1.18 \pm 0.15$	–
	$f_{Z_b(10650)}$	–	–	–	$0.05 \pm 0.04$	$0.24 \pm 0.11$	–
	$\phi_{Z_b(10650)}$ , rad.	–	–	–	$-0.26 \pm 0.68$	$-1.63 \pm 0.14$	–
	$f_{\text{nr}}$	–	$0.48 \pm 0.23$	$0.41 \pm 0.17$	–	–	1.0
	$\phi_{\text{nr}}$ , rad.	–	$-1.21 \pm 0.19$	$0.95 \pm 0.32$	–	–	–
	$-2 \log \mathcal{L}$	–304.7	–300.6	–300.5	–301.4	–301.4	–344.5
$B^*B^*\pi$	$f_{Z_b(10650)}$	1.0	$1.04 \pm 0.15$	$0.77 \pm 0.22$	–	–	–
	$f_{\text{nr}}$	–	$0.02 \pm 0.04$	$0.24 \pm 0.18$	–	–	1.0
	$\phi_{\text{nr}}$ , rad.	–	$0.29 \pm 0.10$	$1.10 \pm 0.44$	–	–	–
	$-2 \log \mathcal{L}$	–182.4	–182.4	–182.4	–	–	–209.7

We first analyze the  $BB^*\pi$  [ $B^*B^*\pi$ ] data with the simplest hypothesis, Model-0, that includes only the  $Z_b(10610)$  [ $Z_b(10650)$ ] amplitude. Results of the fit are shown in Fig. 2; the numerical results are summarized in Table I. The fraction  $f_X$  of the total three-body signal attributed to a particular quasi-two-body intermediate state is calculated as  $f_X = \int |\mathcal{A}_X|^2 dm / \int S(m) dm$ , where  $\mathcal{A}_X$  is the amplitude for a particular component  $X$  of the three-body amplitude. Next, we extend the hypothesis to include a possible non-resonant component, Model-1, and repeat the fit to the data. Then the  $BB^*\pi$  data is fit to a combination of two  $Z_b$  amplitudes, Model-2. In both cases, the addition of an extra component to the amplitude does not give a statistically significant improvement in the data description: the likelihood value is only marginally improved (see Table I). The addition of extra components to the amplitude also produces multiple maxima in the likelihood function. As a result, we use Model-0 as our nominal hypothesis. Finally, we fit both samples to a pure non-resonant amplitude (Model-3). In this case, the fit is significantly worse.

If the parameters of the  $Z_b$  resonances are allowed to float, the fit to the  $BB^*\pi$  data with Model-0 gives  $10605 \pm 6$  MeV/ $c^2$  and  $25 \pm 7$  MeV for the  $Z_b(10610)$  mass and width, respectively, and the fit to the  $B^*B^*\pi$  data gives  $10648 \pm 13$  MeV/ $c^2$  and  $23 \pm 8$  MeV for the  $Z_b(10650)$  mass and width, respectively. The large errors here reflect the strong correlation between the resonance parameters.

The three-body Born cross sections are calculated as

$$\sigma(e^+e^- \rightarrow f) = \frac{N_f}{L \mathcal{B}_f \alpha \eta (1 + \delta_{\text{ISR}}) |1 - \Pi|^2}, \quad (3)$$

where  $N_f$  is the three-body signal yield and  $L = 121.4 \text{ fb}^{-1}$  is the total integrated luminosity. The efficiency-weighted sum of  $B$ -meson branching fractions  $\mathcal{B}_f$  is determined using both signal MC and two-body  $e^+e^- \rightarrow B^{(*)}\bar{B}^{(*)}$  events in data. To avoid the large systematic uncertainties associated with the determination of reconstruction efficiencies for  $B$  and  $D$  decays to multibody final states, we select a subset of two-body

modes:  $B^+ \rightarrow \bar{D}^0[K^+\pi^-]\pi^+$  and  $B \rightarrow J/\psi[\ell^+\ell^-]K$ , and calculate  $\mathcal{B}_f = \mathcal{B}_f^{\text{sel}} \times N_{B^{(*)}\bar{B}^{(*)}}^{\text{all}} / N_{B^{(*)}\bar{B}^{(*)}}^{\text{sel}}$ , where the superscripts “sel” and “all” refer to quantities determined for the selected subset of  $B$  decay modes and for the full set of modes, respectively. Two-body  $e^+e^- \rightarrow B^{(*)}\bar{B}^{(*)}$  events are selected with the requirement  $0.90 \text{ GeV}/c < P(B) < 1.35 \text{ GeV}/c$ ; the  $B$  yield is determined from the fit to the  $M(B)$  distribution. We find  $N_{B^{(*)}\bar{B}^{(*)}}^{\text{all}} = 10131 \pm 152$  and  $N_{B^{(*)}\bar{B}^{(*)}}^{\text{sel}} = 2406 \pm 62$ . (MC studies show no significant dependence of the reconstruction efficiency on the  $B$  momentum.) To account for the non-uniform distribution of signal events over the phase space, we introduce an efficiency correction factor  $\eta$  determined from the MC simulation with signal events generated according to the nominal model. Since we do not observe a signal in the  $BB\pi$  final state, no correction is made for this channel. A factor  $\alpha = 0.897 \pm 0.002$  is introduced to correct for the effect of neutral  $B$ -meson oscillations that is determined using the known  $B^0$  mixing parameter  $x_d$  and the yield ratio in data of two-body events with a reconstructed neutral vs. charged  $B$  meson. The ISR correction,  $1 + \delta_{\text{ISR}}$ , for the  $B^{(*)}B^*\pi$  final states is calculated using recent results on  $\sigma(e^+e^- \rightarrow h_b(mP)\pi^+\pi^-)$  [15] and an observation that the  $\Upsilon(5S) \rightarrow h_b(mP)\pi^+\pi^-$  transitions are saturated by the intermediated  $Z_b$  production [1]; for the  $BB\pi$  final state we assume constant cross section. For the vacuum polarization correction we use  $1/|1 - \Pi|^2 = 0.928$  [16]. The results are summarized in Table II.

TABLE II: Summary of results on three-body cross sections. The first (or sole) uncertainty is statistical; the second is systematic.

Parameter	$BB\pi$	$BB^*\pi$	$B^*B^*\pi$
$N_f$ , Events	$13 \pm 25$	$357 \pm 30$	$161 \pm 21$
$\mathcal{B}_f$ , $10^{-6}$	$293 \pm 22$	$276 \pm 21$	$223 \pm 17$
$\eta$	1.0	1.066	1.182
$1 + \delta_{\text{ISR}}$	$0.720 \pm 0.017$	$0.598 \pm 0.016$	$0.594 \pm 0.016$
$\sigma$ , pb	$< 2.9$	$17.4 \pm 1.6 \pm 1.9$	$8.75 \pm 1.15 \pm 1.04$

TABLE III:  $B$  branching fractions for the  $Z_b^+(10610)$  and  $Z_b^+(10650)$  decays. The first quoted uncertainty is statistical; the second is systematic.

Channel	Fraction, %	
	$Z_b(10610)$	$Z_b(10650)$
$\Upsilon(1S)\pi^+$	$0.54^{+0.16+0.11}_{-0.13-0.08}$	$0.17^{+0.07+0.03}_{-0.06-0.02}$
$\Upsilon(2S)\pi^+$	$3.62^{+0.76+0.79}_{-0.59-0.53}$	$1.39^{+0.48+0.34}_{-0.38-0.33}$
$\Upsilon(3S)\pi^+$	$2.15^{+0.55+0.60}_{-0.42-0.43}$	$1.63^{+0.33+0.33}_{-0.42-0.28}$
$h_b(1P)\pi^+$	$3.45^{+0.87+0.86}_{-0.71-0.63}$	$8.41^{+2.43+1.49}_{-2.12-1.06}$
$h_b(2P)\pi^+$	$4.67^{+1.24+1.18}_{-1.00-0.89}$	$14.7^{+3.2+2.8}_{-2.8-2.3}$
$B^+\bar{B}^{*0} + \bar{B}^0B^{*+}$	$85.6^{+1.5+1.5}_{-2.0-2.1}$	—
$B^{*+}\bar{B}^{*0}$	—	$73.7^{+3.4+2.7}_{-4.4-3.5}$

The dominant sources of systematic uncertainties for the three-body production cross sections are the uncertainties in the signal yield extraction (6.9% for  $BB^*\pi$  and 8.7% for  $B^*B^*\pi$ ), in the reconstruction efficiency (7.6%) (including secondary branching fractions [11]), in the correction factor  $\alpha$  (1%), in the integrated luminosity (1.4%) and in the ISR correction (2.7%). The overall systematic uncertainties for the three-body cross sections are estimated to be 7.9%, 10.8%, and 12.0% for the  $BB\pi$ ,  $BB^*\pi$ , and  $B^*B^*\pi$  final states, respectively.

Using the results of the fit to the  $M_{\text{miss}}(\pi)$  spectra with the nominal model (Model-0 in Table I) and the results of the analyses of  $e^+e^- \rightarrow \Upsilon(nS)\pi^+\pi^-$  [1] and  $e^+e^- \rightarrow h_b(mP)\pi^+\pi^-$  [15, 17], we calculate the ratio of the branching fractions  $\mathcal{B}(Z_b^+(10610) \rightarrow \bar{B}^0B^{*+} + B^+\bar{B}^{*0})/\mathcal{B}(Z_b^+(10610) \rightarrow \text{bottomonium}) = 5.93^{+0.99+1.01}_{-0.69-0.73}$  and  $\mathcal{B}(Z_b^+(10650) \rightarrow B^{*+}\bar{B}^{*0})/\mathcal{B}(Z_b^+(10650) \rightarrow \text{bottomonium}) = 2.80^{+0.69+0.54}_{-0.40-0.36}$ . We also calculate the relative fractions for  $Z_b$  decays, assuming that they are saturated by the already observed  $\Upsilon(nS)\pi$ ,  $h_b(mP)\pi$ , and  $B^{(*)}B^*$  channels. The results are presented in Table III.

To summarize, we report the first observations of the three-body  $e^+e^- \rightarrow BB^*\pi$  and  $e^+e^- \rightarrow B^*B^*\pi$  processes with a statistical significance above  $8\sigma$ . Measured Born cross sections are  $\sigma(e^+e^- \rightarrow [B\bar{B}^* + \text{c.c.}]^\pm\pi^\mp) = (17.4 \pm 1.6 \pm 1.9)$  pb and  $\sigma(e^+e^- \rightarrow [B^*\bar{B}^*]^\pm\pi^\mp) = (8.75 \pm 1.15 \pm 1.04)$  pb. For the  $e^+e^- \rightarrow BB\pi$  process, we set a 90% confidence level upper limit of  $\sigma(e^+e^- \rightarrow [B\bar{B}]^\pm\pi^\mp) < 2.9$  pb. The analysis of the  $B^{(*)}B^*$  mass spectra indicates that the total three-body rates are dominated by the intermediate  $e^+e^- \rightarrow Z_b(10610)^\mp\pi^\pm$  and  $e^+e^- \rightarrow Z_b(10650)^\mp\pi^\pm$  transitions for the  $BB^*\pi$  and  $B^*B^*\pi$  final states, respectively.

We thank the KEKB group for excellent operation of the accelerator; the KEK cryogenics group for efficient solenoid operations; and the KEK computer group, the NII, and PNNL/EMSL for valuable computing and SINET4 network support. We acknowledge support from MEXT, JSPS and Nagoya's TLPRC (Japan); ARC

and DIISR (Australia); FWF (Austria); NSFC (China); MSMT (Czechia); CZF, DFG, and VS (Germany); DST (India); INFN (Italy); MEST, NRF, GSDC of KISTI, and WCU (Korea); MNiSW and NCN (Poland); MES and RFAAE (Russia); ARRS (Slovenia); IKERBASQUE and UPV/EHU (Spain); SNSF (Switzerland); NSC and MOE (Taiwan); and DOE and NSF (USA).

- [1] A. Bondar *et al.* (Belle Collaboration), Phys. Rev. Lett. **108**, 122001 (2012).
- [2] A. Garmash *et al.* (Belle Collaboration), Phys. Rev. D **91**, 072003 (2015).
- [3] D.-Y. Chen and X. Liu, Phys. Rev. D **84**, 094003 (2011); A. Ali, C. Hambrook and W. Wang, Phys. Rev. D **85**, 054011 (2012); I. V. Danilkin, V. D. Orlovsky and Y. A. Simonov, Phys. Rev. D **85**, 034012 (2012); S. Ohkoda, Y. Yamaguchi, S. Yasui, K. Sudoh and A. Hosaka, Phys. Rev. D **86**, 014004 (2012); E. Braaten, C. Langmack and D. H. Smith, Phys. Rev. D **90**, 014044 (2014).
- [4] A. E. Bondar, A. Garmash, A.I. Milstein, R. Mizuk, and M.B. Voloshin, Phys. Rev. D **84**, 054010 (2011).
- [5] A. Drutskoy *et al.* (Belle Collaboration), Phys. Rev. D **81**, 112003 (2010).
- [6] A. Abashian *et al.* (Belle Collaboration), Nucl. Instrum. Methods Phys. Res. Sect. A **479**, 117 (2002); also see detector section in J. Brodzicka *et al.* Prog. Theor. Exp. Phys. 04D001 (2012).
- [7] S. Kurokawa and E. Kikutani, Nucl. Instrum. Methods Phys. Res. Sect. A **499**, 1 (2003), and other papers included in this Volume; T. Abe *et al.* Prog. Theor. Exp. Phys. (2013) 03A001 and following articles up to 03A011.
- [8] D.J. Lange, Nucl. Instrum. Methods Phys. Res. Sect. A **462**, 152 (2001).
- [9] R. Brun *et al.*, GEANT 3.21, CERN Report DD/EE/84-1 (1984).
- [10] D. Liventsev *et al.* (Belle Collaboration) Phys. Rev. D **77**, 091503(R) (2008).
- [11] K.A. Olive *et al.* (Particle Data Group), Chin. Phys. C, **38**, 090001 (2014).
- [12] Determined from the requirement of equal number of events in the RS and WS samples in the  $5.0 \text{ GeV}/c^2 < M_{\text{miss}} < 5.24 \text{ GeV}/c^2$  region in data.
- [13] The bin-by-bin information is available in the on-line supplementary material.
- [14] Determined using mixing parameter  $x_d$  and the ratio of charged to neutral  $B$  yields measured in data from two-body  $e^+e^- \rightarrow B^{(*)}B^{(*)}$  processes. Renormalization factor of  $1.19 \pm 0.01$  is also applied.
- [15] A. Abdesselam *et al.* (Belle Collaboration), arXiv:1508.06562. To be submitted to PRL.
- [16] S. Actis *et al.*, Eur. Phys. J. C **66**, 585 (2010).
- [17] The fits to the  $M_{\text{miss}}(\pi)$  distributions performed in Ref. [1] give fractions of  $f_{Z(10610)^\pm\pi^\mp} = 0.423^{+0.05+0.007}_{-0.127-0.009}$  ( $0.352^{+0.156+0.001}_{-0.004-0.134}$ ) and  $f_{Z(10650)^\pm\pi^\mp} = 0.602^{+0.103+0.11}_{-0.211-0.038}$  ( $0.648^{+0.152+0.067}_{-0.114-0.155}$ ) for the  $h_b(1P)$  ( $h_b(2P)$ ) decays.